nature synthesis

Supplementary information

https://doi.org/10.1038/s44160-024-00661-y

Mechanochemical nitrogen fixation catalysed by molybdenum complexes

In the format provided by the authors and unedited

Table of Contents

General Methods.

^{1}H NMR (400 MHz) and ^{31}P{^{1}H} NMR (162 MHz) spectra were recorded on a JEOL ECS-400 spectrometer in a suitable solvent, and spectra were referenced to residual solvent (^{1}H) or external standard (^{31}P{^{1}H}: 85% H_3PO_4). Electrospray ionization time-of-flight mass (ESI-TOF-MS) spectra were recorded on a JEOL Accu TOF JMS-T100LP. Elemental analyses were performed at Microanalytical Center of The University of Tokyo. Ultraviolet–visible (UV–vis) absorption spectra for indophenol method[S1] and *p*-(dimethylamino)benzaldehyde method[S2] were recorded on a Shimadzu UV-1850. UV-vis diffuse reflectance spectra were recorded on Shimadzu UV-2600i equipped with integrating sphere. FT-IR spectrum for detection of gas-phase NH_3 was recorded on a JASCO FT/IR 4100 Fourier transform infrared spectrometer equipped with 10 cm gas cell with CaF_2 window. ATR-IR spectra were recorded on a Shimadzu IR Spirit equipped with a QATR-S ATR unit. Evolved dihydrogen (H_2) was quantified by a gas chromatography (GC) using a Shimadzu GC-8A with a TCD detector and SHINCARBON ST (6 m × 3 mm). Powder X-ray diffraction (PXRD) measurements were performed on a Rigaku MiniFlex600 equipped with a 600 W Cu anode (Cu*K*α, λ = 1.54 Å). Mechanochemical reactions were performed using Retsch MM400 grinding vessels (Supplementary Fig. 1). Both jars and balls were made of stainless steel (Supplementary Fig. 2). Homogeneous reactions using solvents were carried out under an atmosphere of nitrogen (N_2) or argon (Ar) by using standard Schlenk techniques or glovebox techniques unless otherwise stated. Solvents were dried by general methods and degassed before use. Pentaerythritol-d_4[S3], [MoI_3(PCP)] (**1a**, PCP = 1,3-bis(di-*tert*-butylphosphinomethyl)benzimidazol-2-ylidene)[S4], [MoI_3(CF_3-PCP)] (**1b**, CF_3-PCP = 1,3-bis(di-*tert*-butylphosphinomethyl)-5-trifluoromethylbenzimidazol-2-ylidene)[S5], [Mo(N)I(PCP)] (**2**)[S5], [MoI_3(PNP)] (**3**, PNP = 2,6-bis(di-*tert*-butylphosphinomethyl)pyridine)[S6], *trans*-[$Mo(N_2)_2(PPh_2Me)_4$] (**4**)[S7], *trans*-[$Mo(N_2)_2$(dppe)$_2$] (**5**, dppe = 1,2-bis-(diphenylphosphino)ethane)[S8], and $SmI_2(thf)_2$[S9] were prepared according to the literature methods. Pentaerythritol (TCI), cellulose (Wako, powder, <38 μm), and the other non-volatile alcohols were purchased commercially and dried by heating at 110 °C under vacuum overnight prior to use. Other reagents were purchased commercially and used as received.

Experimental Section.

Synthesis and characterization of pentaerythritol-d_4. The synthesis of pentaerythritol-d_4 was carried out according to the modified literature method[S3]. Pentaerythritol (600 mg) was dissolved in D_2O (24 mL) and evaporated to dryness. This process was repeated for three times to give pentaerythritol-d_4. For kinetic isotope effect measurements, pentaerythritol was prepared by the similar procedures as the preparation of pentaerythritol-d_4, where H_2O was used instead of D_2O. Pentaerythritol and pentaerythritol-d_4 was subjected to elemental analysis to confirm their composition. (Pentaerythritol: Calcd: C, 44.1; H, 8.88; Found C, 44.08; H, 8.49. Pentaerythritol-d_4: Calcd. C: 42.84, Found C: 42.85.)

Synthesis of [MoI_3(PCP)] (1a). [MoI_3(PCP)] was prepared according to the literature method as follows[S4]. To a mixture of 1,3-bis((di-*tert*-butylphosphino)methyl)-1*H*-benzo[*d*]imidazol-3-ium hexafluorophosphate[S8] and $KN(SiMe_3)_2$ was added toluene, and the resulting suspension was stirred at room temperature for 2 h. The suspension was filtered through Celite and the solvent was removed under vacuum. [$MoI_3(thf)_3$][S9] and THF were added to the residue and stirred at 50 °C for 19 h. The resultant solution was filtered and the solvent was removed under vacuum. The residue was washed with Et_2O to afford **1a** as a brown solid.

Synthesis of [MoI_3(CF_3-PCP)] (1b). [MoI_3(CF_3-PCP)] was prepared according to the literature method as follows[S5]. To a cooled solution of 1,3-bis((di-*tert*-butylphosphino)methyl)-6-(trifluoromethyl)-1*H*-benzo[*d*]imidazol-3-ium hexafluorophosphate[S10] in toluene at −78 °C was added $KN(SiMe_3)_2$, and the mixture was stirred at room temperature for 1 h. The mixture was filtered through Celite, and the filter cake was washed with toluene. The solvent was removed under reduced pressure to give as yellow-brown oily solid. To the residue were added [$MoI_3(thf)_3$] and THF, and the mixture was stirred at 50 °C for 16 h. The resultant dark brown solution was filtered, and slow addition of hexane to the filtrate afforded **1b** as a brown crystalline solid.

Synthesis of [Mo(N)I(PCP)] (2). [Mo(N)I(PCP)] was prepared according to the literature method as follows[S5]. To a solution of [MoI_3(PCP)] (**1a**) in THF was added a solution of $CoCp^*_2$[S11] in THF at −78 °C under N_2 (1 atm), and the mixture was stirred at room temperature for 18 h. The resultant yellow-brown suspension was filtered through Celite, and the filter cake was washed with THF. Volatiles were removed in vacuo, and the residue was washed with hexane and dried in vacuo. The resultant yellow-brown solid was extracted with THF, and slow addition of hexane to the extract afforded **2** as yellow-brown crystals.

Synthesis of [MoI_3(PNP)] (3). [$MoI_3(PNP)_3$] was prepared according to the literature method as follows[S6]. A mixture of [$MoI_3(thf)_3$] and PNP (2,6-bis(di-*tert*-butylphosphinomethyl)pyridine)[S12] in THF was stirred at 50 °C for 18 h. The resultant reddish-brown solution was filtered through Celite, and the filter cake was washed with THF. The combined filtrate was concentrated in vacuo, and the residue was washed with Et_2O to afford **3** as a brown solid.

Synthesis of *trans*-[$Mo(N_2)_2(PPh_2Me)_4$] (4). *trans*-[$Mo(N_2)_2(PPh_2Me)_4$] was prepared by the reduction of Mo_2Cl_{10} with magnesium in the presence of PPh_2Me under 1 atm of N_2 in THF at 0 °C[S7].

Synthesis of *trans*-[Mo(N$_2$)$_2$(dppe)$_2$] (5). *trans*-[Mo(N$_2$)$_2$(dppe)$_2$] was prepared according to the literature method as follows[S8]. 1,2-bis-(diphenylphosphino)ethane (dppe) and $MoCl_5$ were dissolved in THF. Then magnesium turnings which had been dried by flame heating in vacuo were added and the reactants were stirred vigorously under N_2 for 16 h. The resulting dark red-orange solution was filtered through Celite to remove the excess of magnesium, concentrated, and then precipitated from solution by adding MeOH. The orange-yellow crystals of **5** were obtained by recrystallisation from THF/MeOH.

Synthesis of SmI$_2$(thf)$_2$. $SmI_2(thf)_2$ was prepared by stirring a mixture of Sm metal and diiodoethane in THF at 60 °C overnight[S9].

Procedures for mechanochemical nitrogen fixation with a small amount of catalyst. For catalytic reactions using a small amount of molybdenum complexes (Table 2, Entries 2, 3, and 5), a slightly modified procedure was adopted to accurately weight the catalysts. A THF solution (10 mL) of [MoI_3(PCP)] (**1a**, 4.6 mg, 5.0 μmol) was prepared. Then, 200 μL of this solution (containing 0.1 μmol of **1a**) was added to a milling jar with a microsyringe. THF in the jar was removed under reduced pressure at room temperature. The following procedures are the same as the typical procedure for catalytic reactions shown above.

Reductions of hydrocarbons. A typical procedure is shown below: In an Ar-filled glovebox, anthracene (21.4 mg, 0.12 mmol), $SmI_2(thf)_2$ (198 mg, 0.36 mmol), pentaerythritol (98.0 mg, 0.72 mmol), and a stainless-steel ball (*d* = 10.0 mm) were added in a stainless-steel milling jar (~5 mL). The jar was tightly capped and placed in a grinding vessel. After grinding by ball milling at 30 Hz for 1 h, the jar was opened in a sealed bag, and generated H_2 was quantified by GC measurements. H_2 was not generated in all the reaction. The reaction mixture in the jar was quenched with dilute hydrochloric acid (1 M, 30 mL), and the organic layer was extracted with dichloromethane (CH_2Cl_2, 30 mL × 3). The combined organic phase was dried with anhydrous magnesium sulphate and the volatiles were removed in vacuo. To the obtained solid was added hexamethylbenzene and $CDCl_3$ to determine the yield of 9,10-dihydroanthracene and the recovery of unreacted anthracene by ^{1}H NMR measurements.

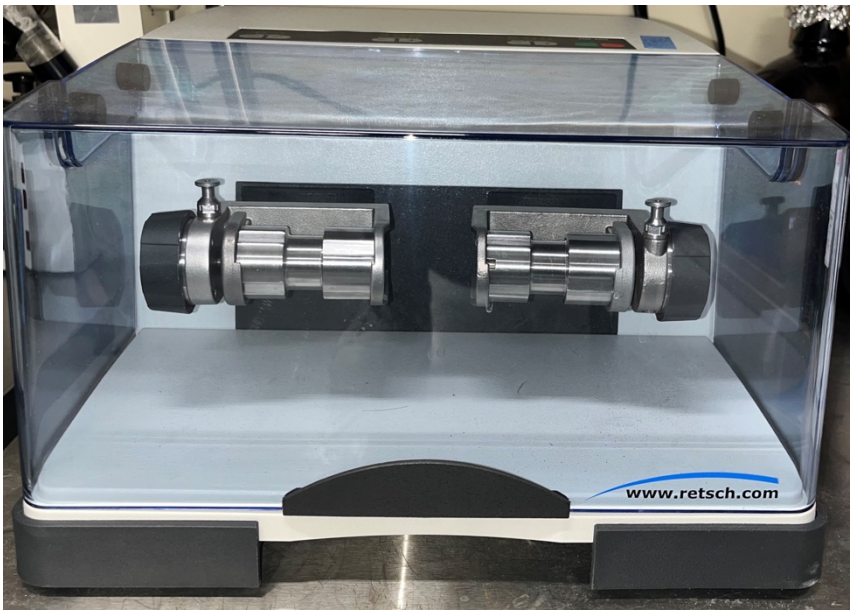

Supplementary Fig. 1 | Photograph of a Retsch MM400 grinding vessel.

Supplementary Fig. 2 | Photograph of Smart Bag PA used for collecting the gas generated by the reaction.

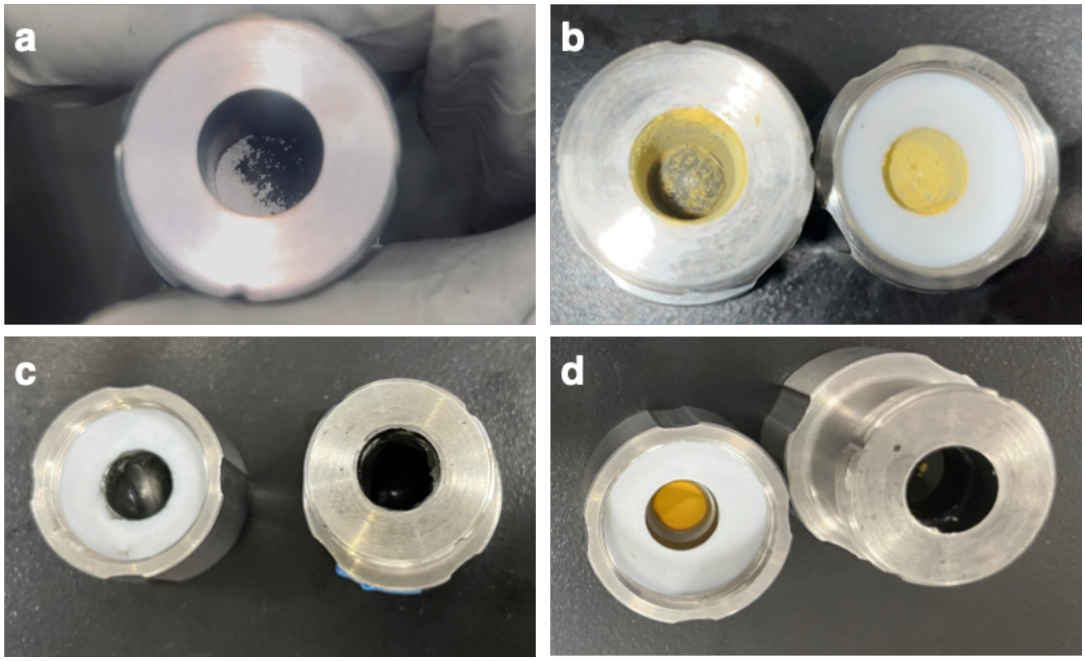

Supplementary Fig. 3 | Photographs of the reactants before and after mechanochemical reactions. **a** Reactants before mechanochemical reaction. **b** the mixture after mechanochemical reaction for 1 h. **c** the mixture after mechanochemical reaction for 1 h in control experiments. **d** the mixture after mechanochemical reaction for 1 h and then left in air until remaining $SmI_2(thf)_2$ was quenched.

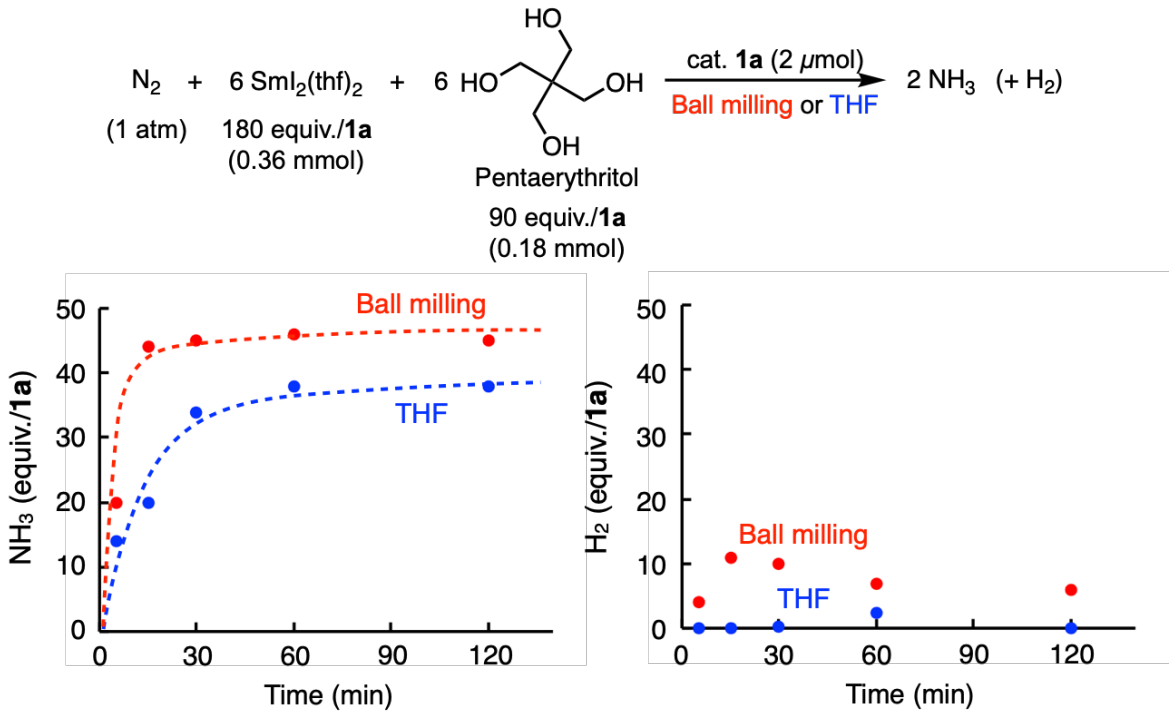

Supplementary Fig. 4 | Time courses of NH_3 and H_2 formation in the mechanochemical nitrogen fixation. An atmospheric pressure of dinitrogen was reacted with $SmI_2(thf)_2$ (0.36 mmol) and pentaerythritol (0.18 mmol) in the presence of **1a** (2 μmol) under either mechanochemical (by ball milling, red) or homogenous (in THF, blue) conditions for 5, 15, 30, 60, or 120 min.

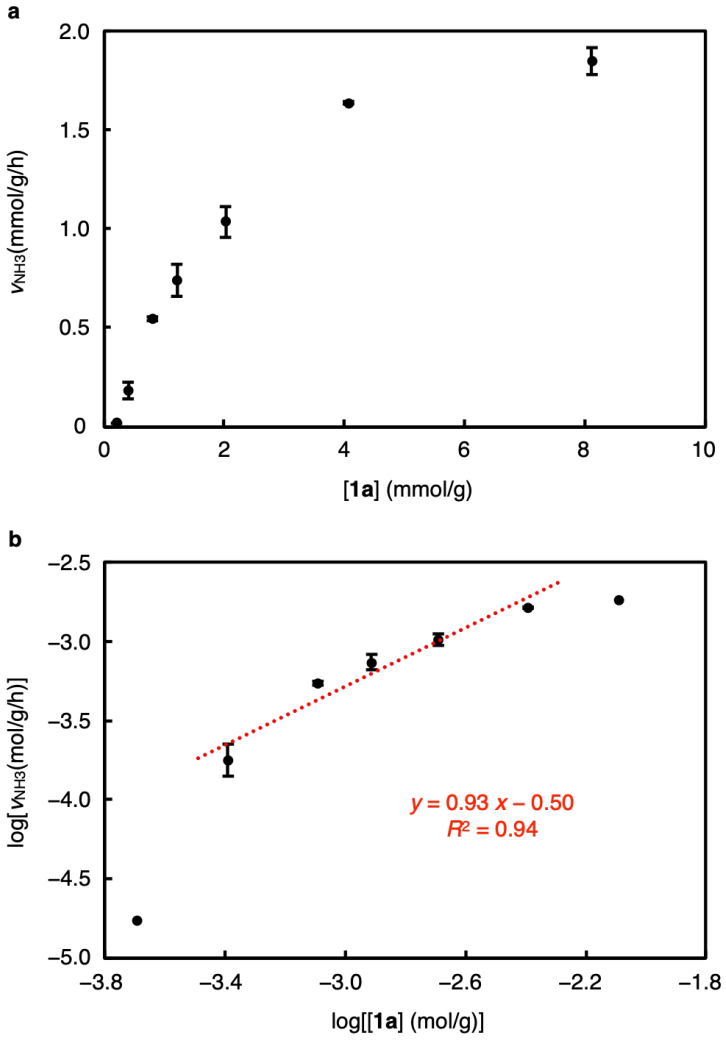

Supplementary Fig. 5 | Catalyst concentration dependency of the reaction rate of mechanochemical nitrogen fixation. **a** An atmospheric pressure of dinitrogen was reacted with $SmI_2(thf)_2$ (197.4 mg, 0.36 mmol) and pentaerythritol (49.0 mg, 0.18 mmol) in the presence of various amount of the catalyst **1a** under mechanochemical conditions. Ammonia formation rates are calculated by (formed ammonia (mmol) / (sample weight = 0.1974 + 0.049 = 0.2464 (g)) / (reaction time (h)). Data are the mean of multiple individual experiments (at least two) with error bars representing standard deviation. Reaction conditions and the results are listed in Supplementary Table 5. **b** Double logarithmic plots of reaction rates against concentrations of **1a**. Data are the mean of multiple individual experiments (at least two) with error bars representing standard deviation. These experimental results indicate the reaction rate of mechanochemical nitrogen fixation follows the 1st order against the catalyst concentration with a certain concentration range in the solid state. The kinetics of the present mechanochemical reaction resembles the solution state reaction we previously reported[S10] involving PCET process as the rate determining step at a higher catalyst concentration. From these reasons, we consider that the PCET process is involved as the rate determining step in the present reaction conditions.

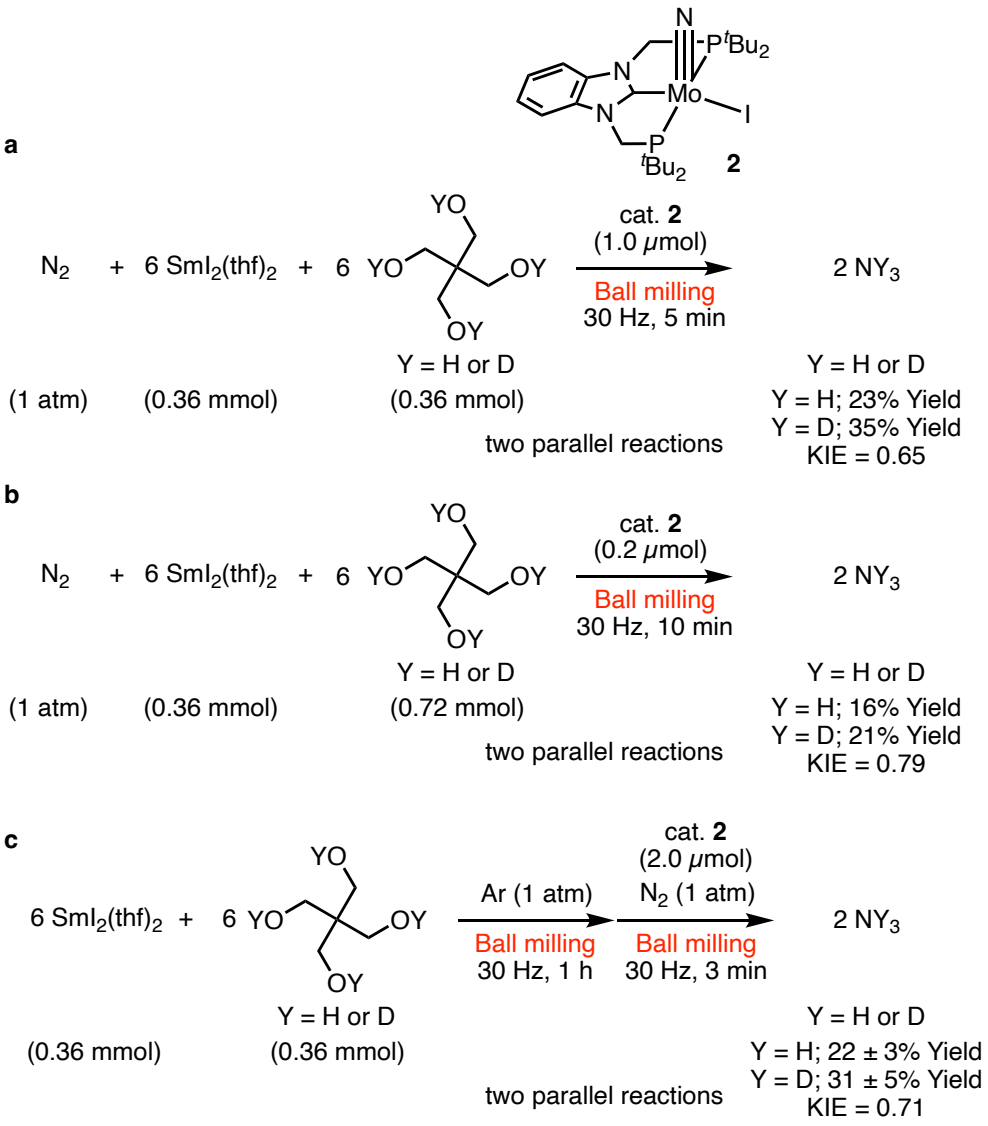

Supplementary Fig. 6 | Isotope labelling experiments to evaluate the Kinetic Isotope Effect (KIE) in the catalytic nitrogen fixation using molybdenum nitride complex 2 under mechanochemical conditions. The inverse kinetic isotope effect (~0.7) was observed in all the cases. Based on these experiments, we suppose that the observed two different types of kinetics are derived from whether O–H bond cleavage and/or E–H (E = N, C) bond formation is involved in the rate-determining step. This suggests that PCET process is involved as the rate determining step in the mechanochemical nitrogen fixation but in a slightly different manner to the hydrocarbon reduction.

Procedures for generation of gaseous NH_3 by adding solid Brønsted base. KOH powder was prepared by grinding KOH pellets in a mortar in an Ar-filled glovebox. Mechanochemical reaction using $SmI_2(thf)_2$ (198 mg, 0.36 mmol), pentaerythritol (49.0 mg, 0.36 mmol), [$MoI_3(CF_3$-PCP)] (**1b**, 0.1 μmol), and a stainless-steel ball (d = 10.0 mm) was carried out under N_2 atmosphere following the typical procedure described above. After the reaction, the jar was opened in an Ar-filled glovebox, and KOH powder (108 mg, 2.7 mmol, 7.5 equiv./Sm) was added to the jar. The jar was tightly capped, placed in a grinding vessel, and again ball milled at 30 Hz for 1 h. After ball milling for 1 h, the amounts of *gas-phase NH_3* (523 equiv./Mo) and *solid-phase NH_3* (11 equiv./Mo) were quantified following the typical procedure.

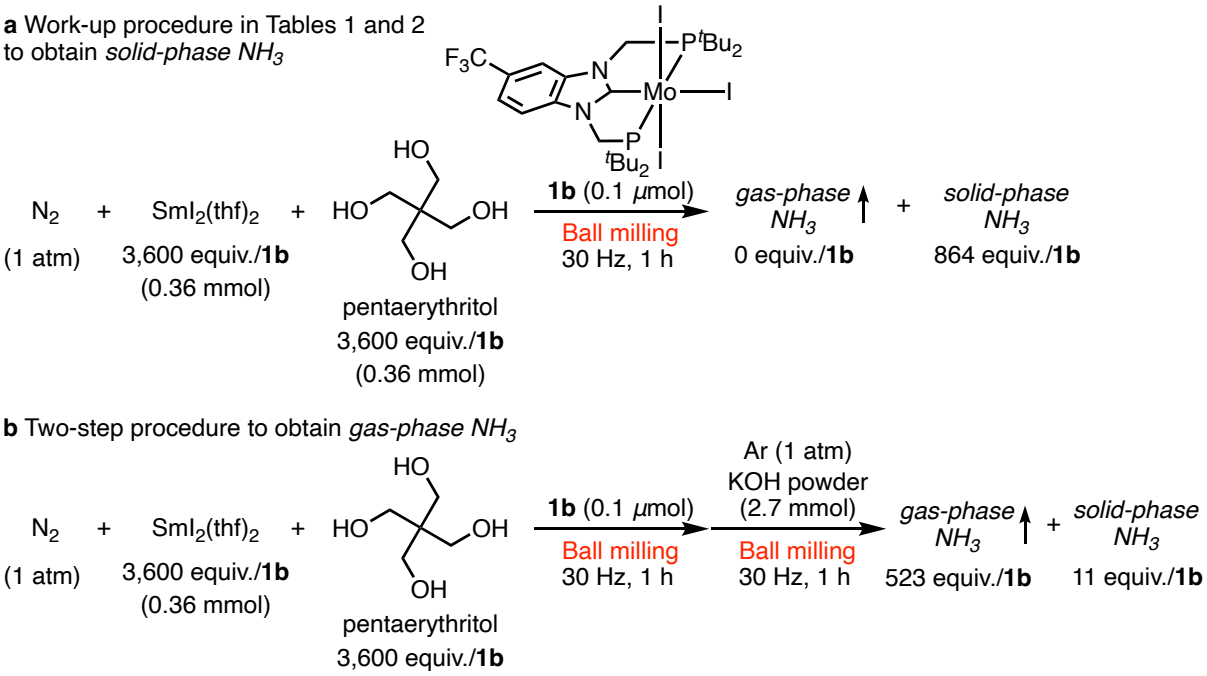

Supplementary Fig. 7 | Generation of gaseous NH_3 by adding solid Brønsted base. **a** Work-up procedure in Tables 1 and 2 to obtain *solid-phase NH_3*. **b** Two-step procedure to obtain *gas-phase NH_3*.

Typical procedures for stoichiometric reactions.

Reduction of 1a under atmospheric pressure of N_2. THF and THF-d_8 were degassed by three freeze-pump-thaw cycles and kept in Ar atmosphere. In a N_2-filled glovebox, complex **1a** (13.5 mg, 15 μmol), 5 equiv. of $SmI_2(thf)_2$ (41.2 mg, 75 μmol), and a stainless-steel ball (d = 10.0 mm) were added in a stainless-steel milling jar (~5 mL). The jar was tightly capped and placed in a grinding vessel. After ball milling at 30 Hz for 10 min, the jar was opened in an Ar-filled glove box, and the resulting reaction mixture was transferred to a 20 mL Schlenk flask with ~ 6 mL of THF. After the volatiles were removed under reduced pressure, hexamethylbenzene (3.0 mg, 0.018 mmol) and 0.8 mL of THF-d_8 were added. The mixture was stirred at room temperature, and ^1H and $^{31}P\{^1H\}$ NMR measurements were conducted (Supplementary Figs. 8 and 9). ^1H and $^{31}P\{^1H\}$ NMR spectra were consistent with the reported data of complex **2**[S5]. ^1H NMR results were used to calculate the yield of complex **2** (34% yield). An aliquot of reaction mixture in THF was subjected to ESI-TOF-MS measurements and peaks suggesting the formation of nitride complex **2** (m/z = 634) were detected (Supplementary Fig. 10).

NH_3 formation by the reaction of nitride complex 2 with SmI_2 and pentaerythritol. In an Ar-filled glove box, complex **2** (10.1 mg, 15 μmol), 5 equiv. of $SmI_2(thf)_2$ (41.2 mg, 75 μmol), 5 equiv. of pentaerythritol (10.2 mg, 75 μmol), and a stainless-steel ball (d = 10.0 mm) were added in a stainless-steel milling jar (~5 mL). The jar was tightly capped and placed in a grinding vessel. After grinding by ball milling at 30 Hz for 1 h, the jar was opened and the amount of *gas-phase NH_3* (0%) and *solid-phase NH_3* (>99%) were quantified following the typical experimental procedure.

NMR Spectra.

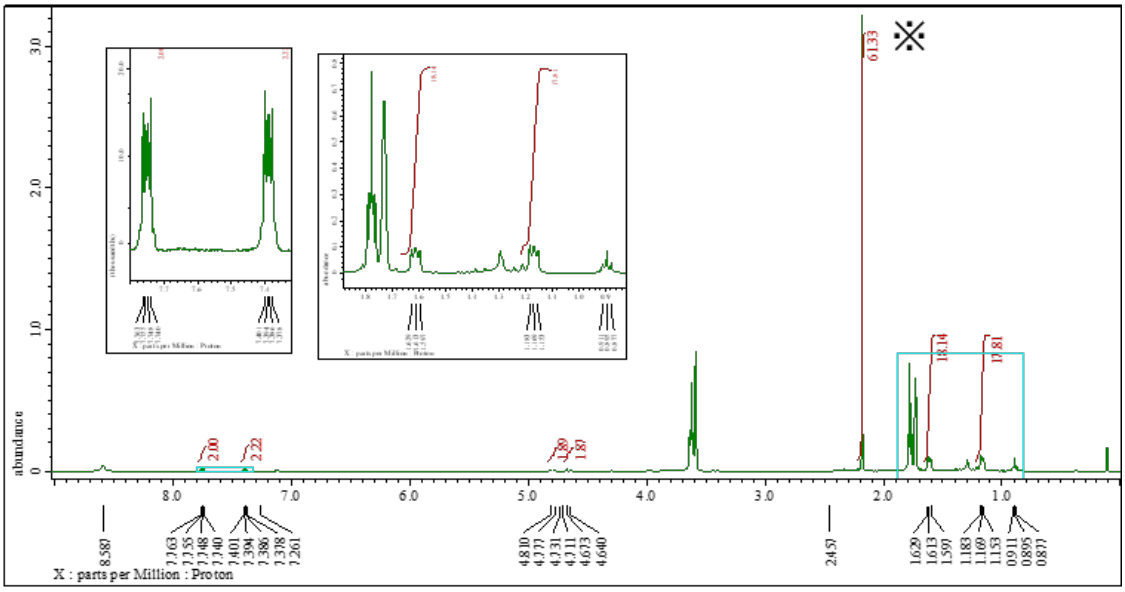

Supplementary Fig. 8 | ^{1}H NMR spectrum (THF-d_8) after mechanochemical reaction of 1a with 5 equiv. of $SmI_2(thf)_2$ under mechanochemical conditions. A peak with asterisk indicates the internal standard.

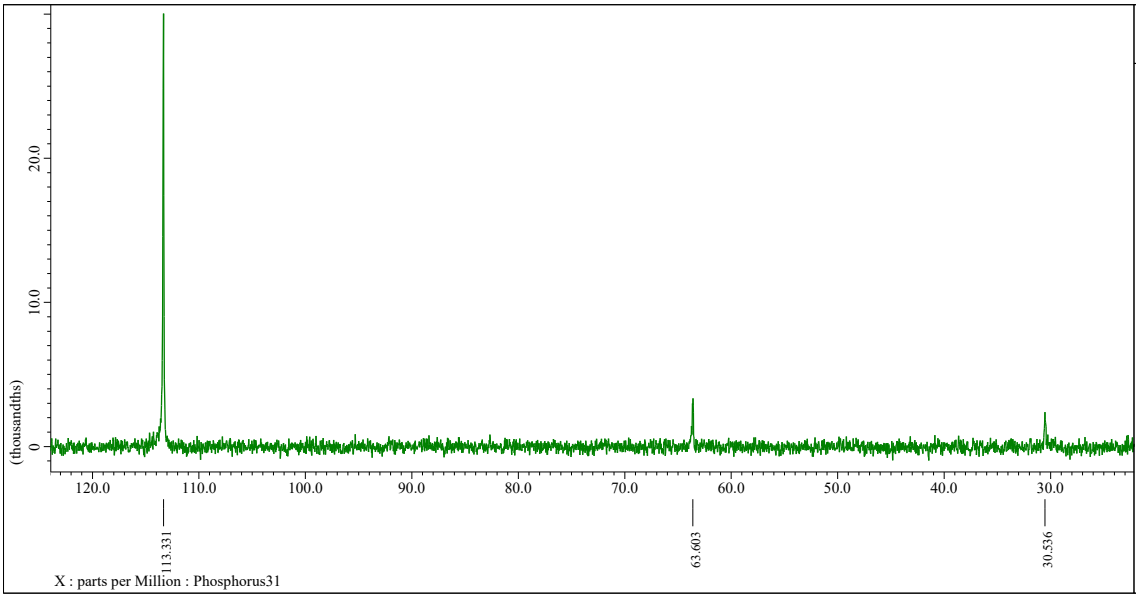

Supplementary Fig. 9 | ^{31}P{^{1}H} NMR spectrum (THF-d_8) after stoichiometric reaction of 1a with 5 equiv. of $SmI_2(thf)_2$ under mechanochemical conditions.

ESI-TOF-MS Spectra.

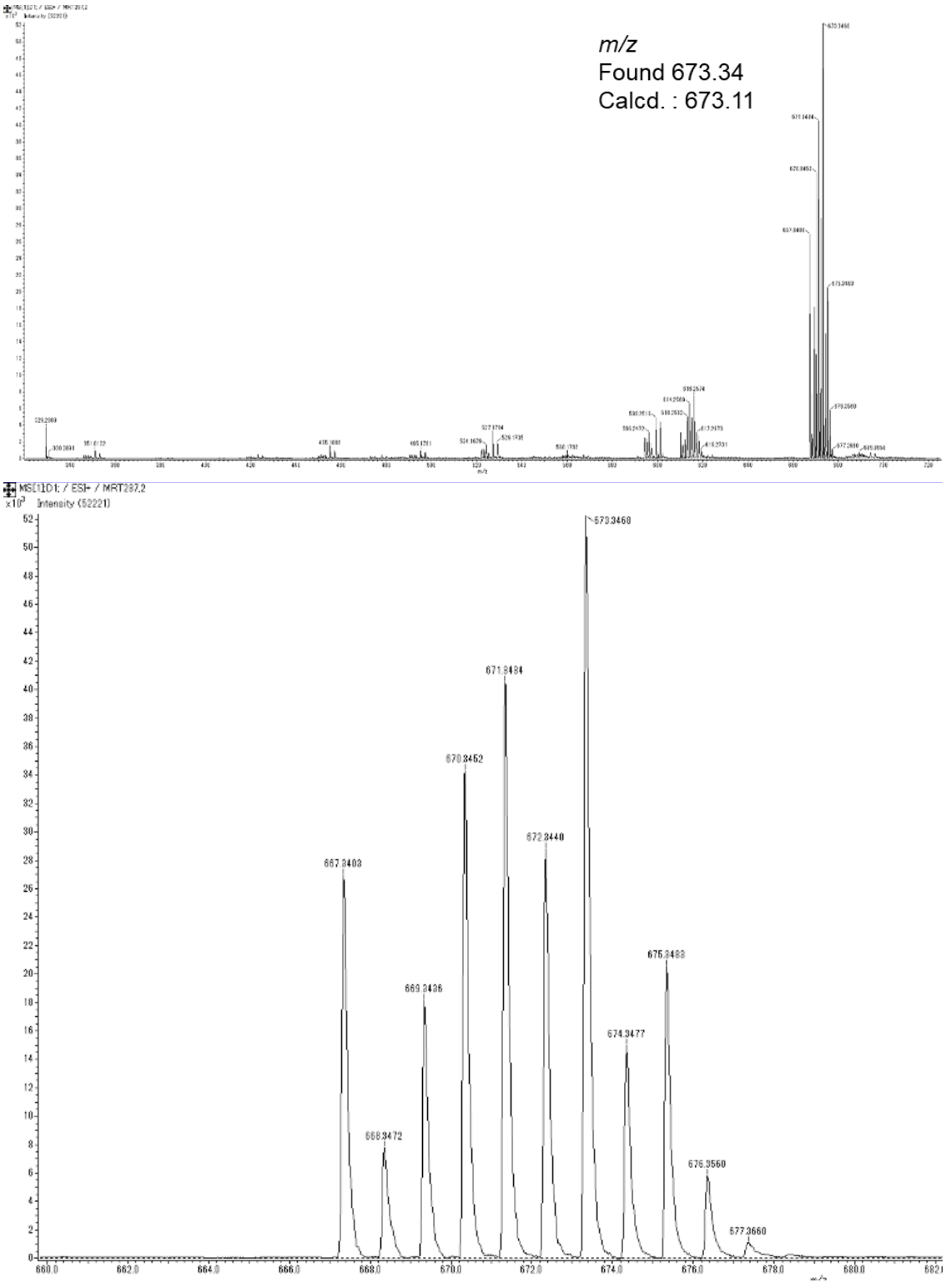

Supplementary Fig. 10 | ESI-TOF-MS spectrum after stoichiometric reaction of 1a with 5 equiv. of $SmI_2(thf)_2$.
(top: overall view, bottom: enlarged view.)

XAS Spectra.

Sample preparation for X-ray absorption (XAS) measurements. Mechanochemical reaction of complex **1a** (42.3 mg, 0.046 mmol) with 5 equiv. of $SmI_2(thf)_2$ (127.2 mg, 0.23 mmol) using a stainless-steel ball (d = 10.0 mm) under N_2 atmosphere was carried out as described in the typical procedure above. After the reaction, the jar was opened in an Ar-filled glovebox and the solid reaction mixture was collected with spatula. Boron nitride (115 mg) was mixed with the reaction mixture using a mortar and processed into pellets (diameter: 7 mm). The pellets were sealed in aluminium bags (LAMIZIP, SEISANNIPPONSHA LTD.) and taken out of the glovebox. Mo K-edge XAS spectra were measured in a transmission mode at the NW10A beamline of the Photon Factory in the High Energy Accelerator Research Organization (KEK-PF, Japan). The XAS data were analysed using Athena software from Demeter package[S10]. The obtained k^2-weighted EXAFS were Fourier transformed in the k range of 3.0–13.3 Å. Linear combination fitting analysis was performed using the standard normalized spectra of **1a** and **2**.

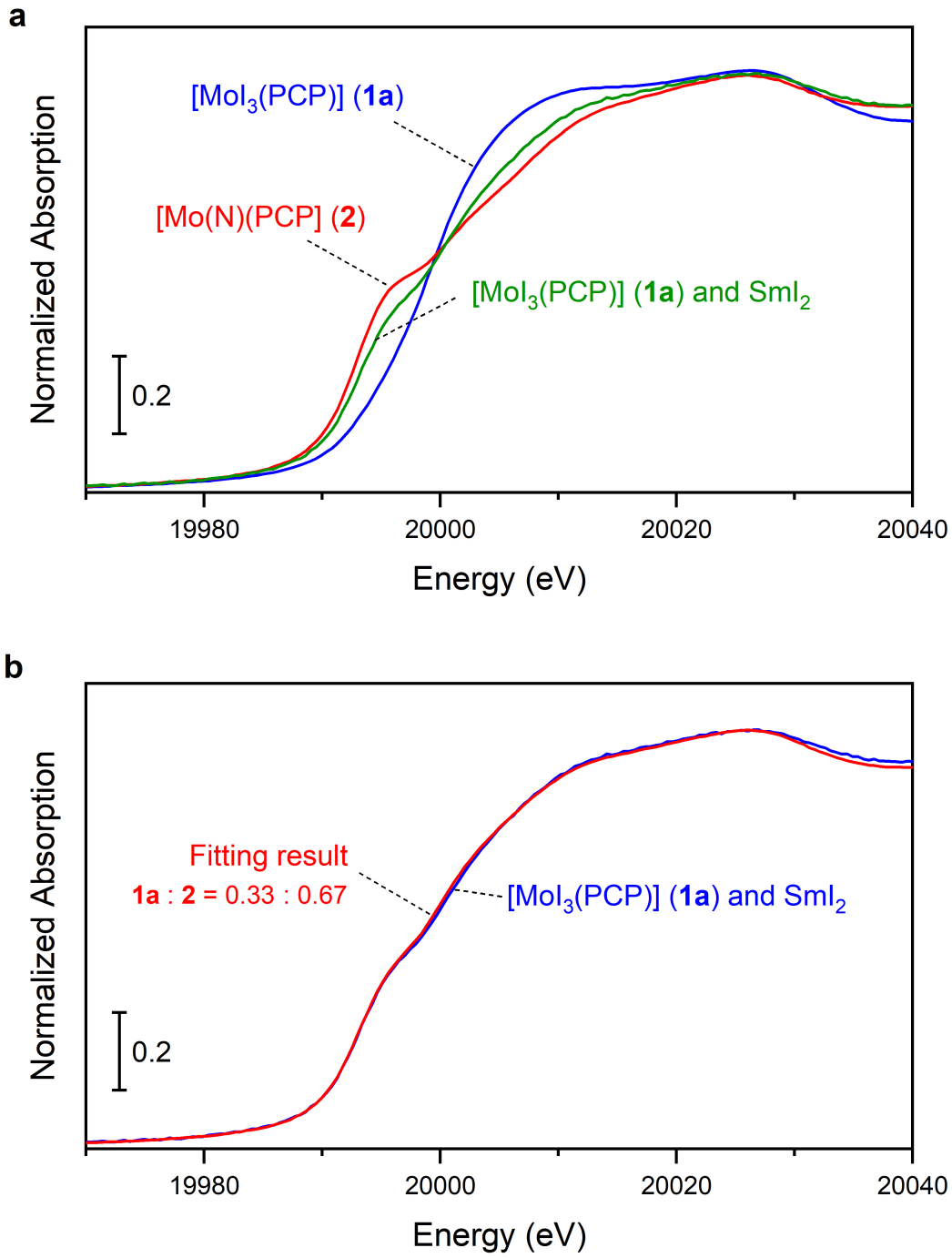

Supplementary Fig. 11 | XANES spectrum of the residue obtained from the reaction of 1a with $SmI_2(thf)_2$. a XANES spectra of complex **1a** (blue), **2** (red), and the reaction mixture (green). **b** Comparison between observed XANES spectrum (blue) and result of linear combination fitting using spectra of **1a** and **2** (red).

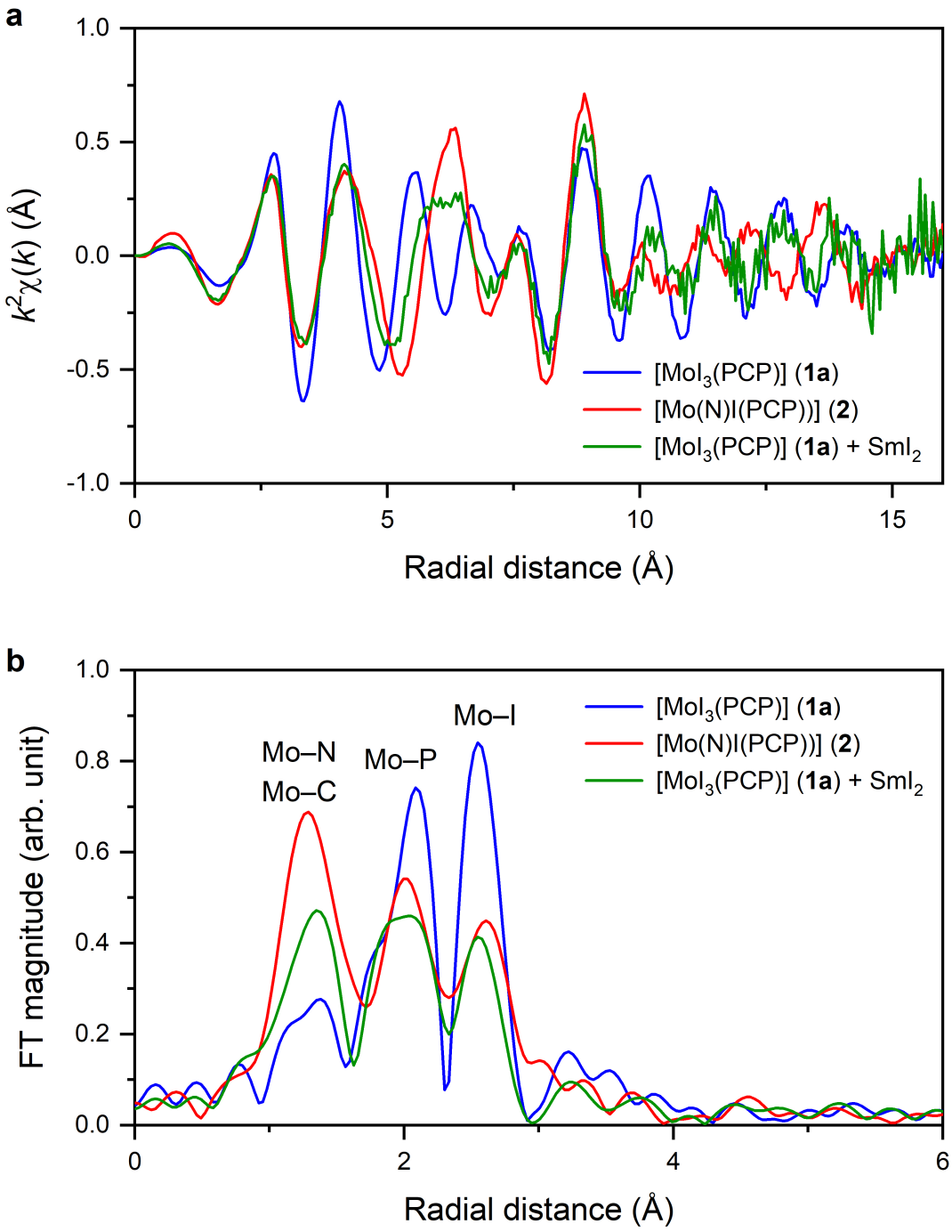

Supplementary Fig. 12 | EXAFS spectrum of the residue obtained from the reaction of 1a with $SmI_2(thf)_2$. a EXAFS spectra of complex **1a** (blue), **2** (red), and the reaction mixture (green). **b** Fourier transform of **a**.

PXRD Patterns.

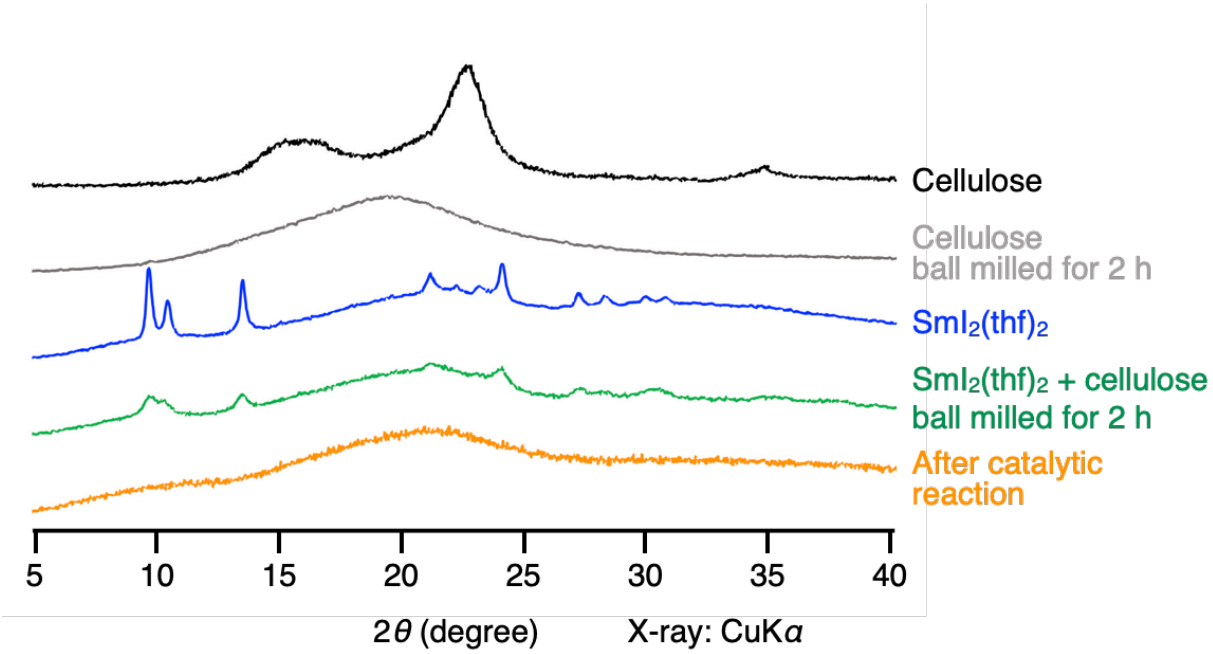

Supplementary Fig. 13 | PXRD patterns of cellulose before and after ball milling.

FT-IR Spectra.

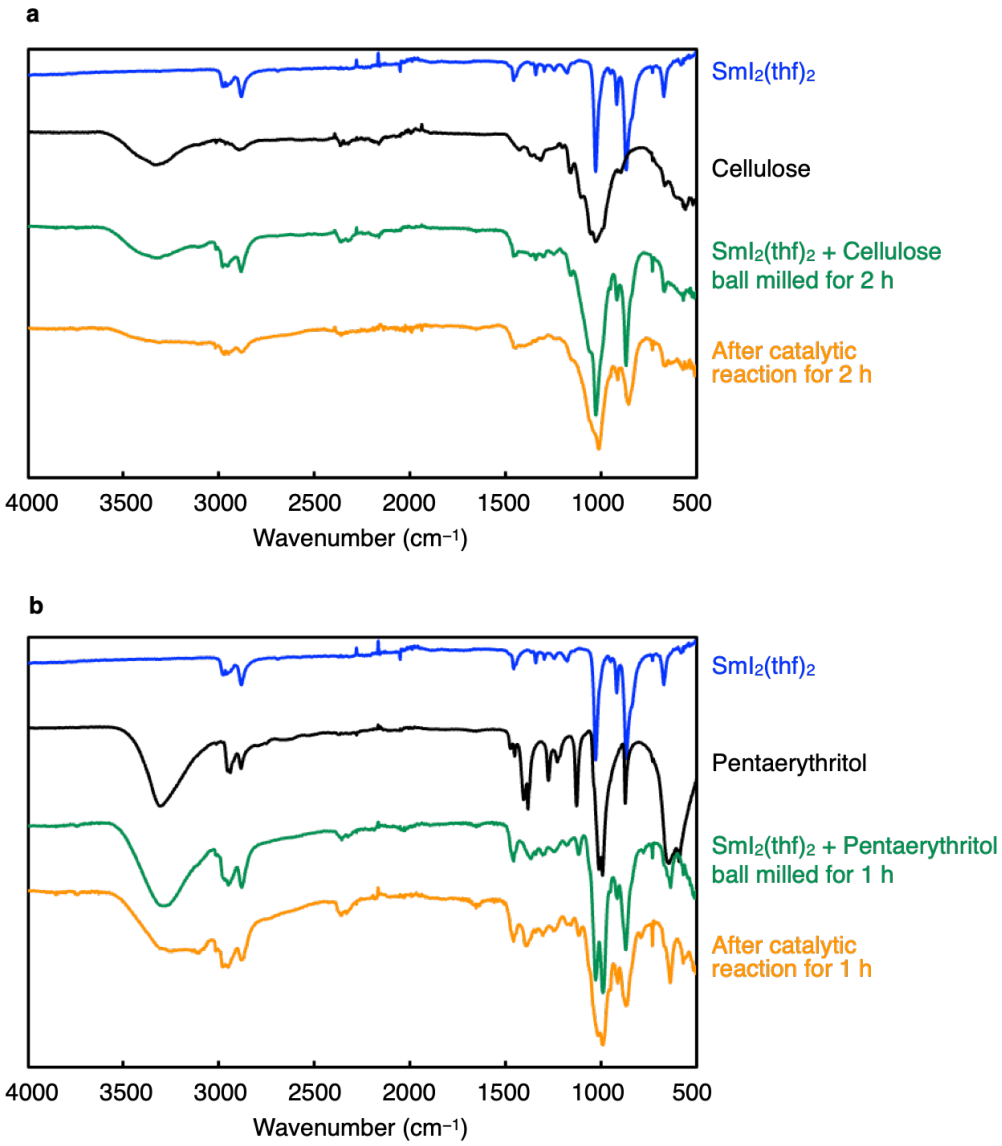

Supplementary Fig. 14 | ATR FT-IR spectra of solid-phase samples. Blue: $SmI_2(thf)_2$. Black: **a** Cellulose or **b** pentaerythritol. Green: The mixtures of $SmI_2(thf)_2$ (0.36 mmol) and **a** cellulose (0.36 mmol) or **b** pentaerythritol (0.36 mmol) ball milled under atmospheric pressure of Ar for 2 h or 1 h, respectively. Orange: The mixtures after the reactions of an atmospheric pressure of dinitrogen with $SmI_2(thf)_2$ (0.36 mmol) and **a** cellulose (0.36 mmol based on $C_6H_{10}O_5$ unit) or **b** pentaerythritol (0.36 mmol) in the presence of the molybdenum catalyst **1a** (2 μmol) under mechanochemical ball-milling conditions for 2 h or 1 h, respectively.

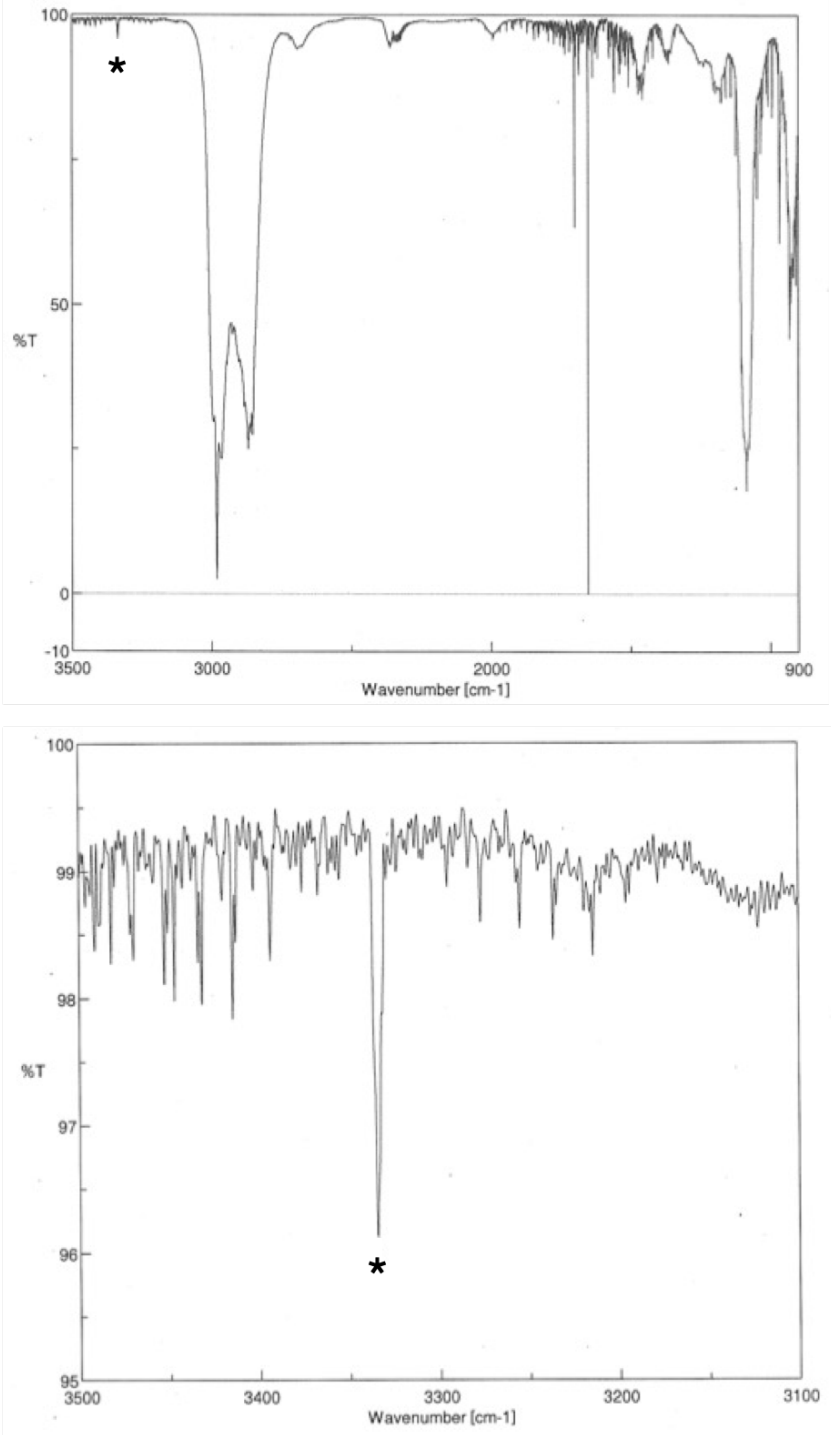

Supplementary Fig. 15 | FT-IR spectrum of gas-phase after catalytic reaction. An atmospheric pressure of dinitrogen was reacted with $SmI_2(thf)_2$ (197.4 mg, 0.36 mmol) and pentaerythritol (49.0 mg, 0.36 mmol) in the presence of the molybdenum catalyst **1a** (2 μmol) under mechanochemical ball-milling conditions followed by ball milling with KOH (150 mg, 2.7 mmol). A peak at 3334 cm^{-1} with asterisk is assignable to the N–H stretching vibration of NH_3 (top: overall view in the range of 900–3500 cm^{-1}, bottom: enlarged view in the range of 3100–3500 cm^{-1}).

UV-Vis Diffuse Reflectance Spectra.

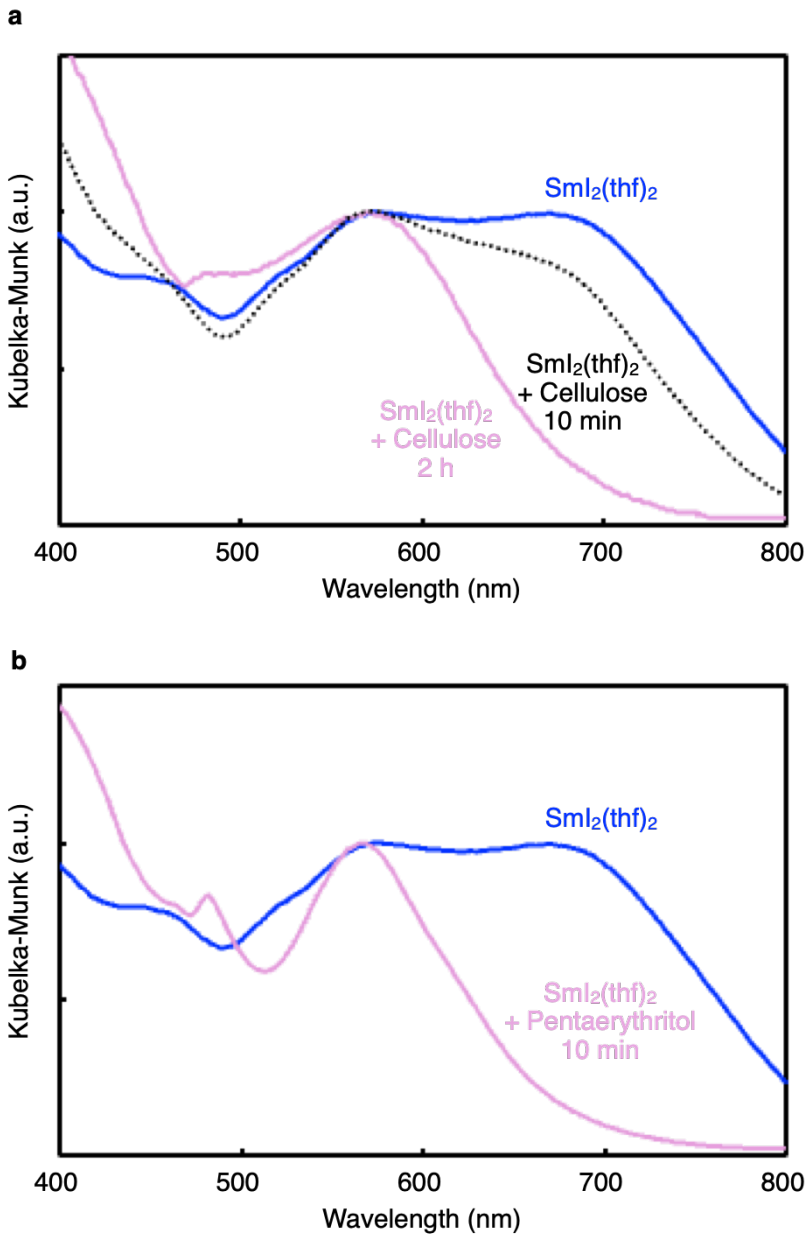

Supplementary Fig. 16 | UV-Vis diffuse reflectance spectra of solid-phase samples. Blue: $SmI_2(thf)_2$. Purple: An atmospheric pressure of dinitrogen was reacted with $SmI_2(thf)_2$ (65.8 mg, 0.12 mmol) and **a** cellulose (194.6 mg, 1.2 mmol) or **b** pentaerythritol (163.4 mg, 1.2 mmol) for 10 min or 2 h under mechanochemical ball-milling conditions.

Gas Chromatogram.

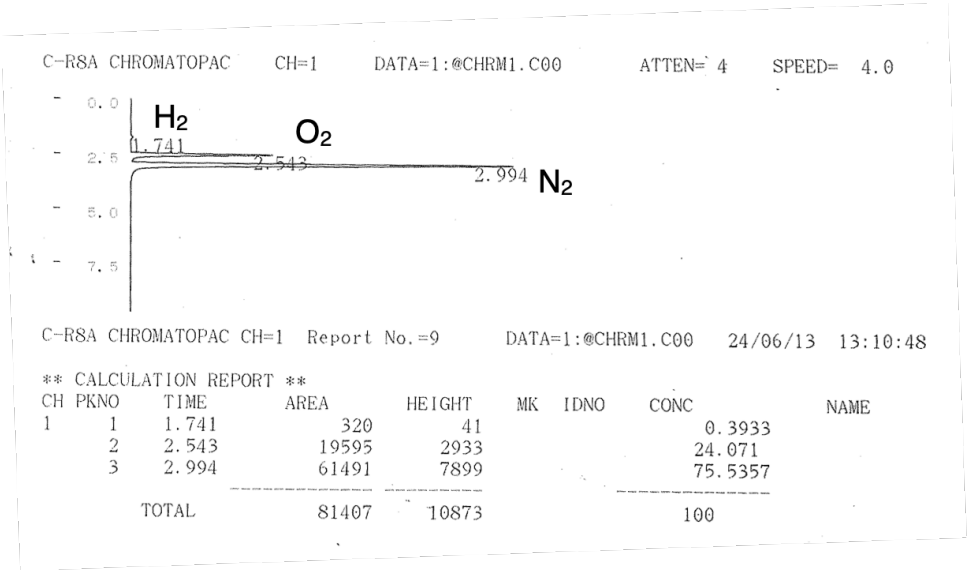

Supplementary Fig. 17 | Typical gas chromatogram of gas-phase after catalytic reaction. An atmospheric pressure of dinitrogen was reacted with $SmI_2(thf)_2$ (0.36 mmol) and pentaerythritol (0.36 mmol) in the presence of the molybdenum catalyst **1a** (2 μmol) under mechanochemical ball-milling conditions.

Supplementary Table 1. Examination of reaction conditions in mechanochemical nitrogen fixation.

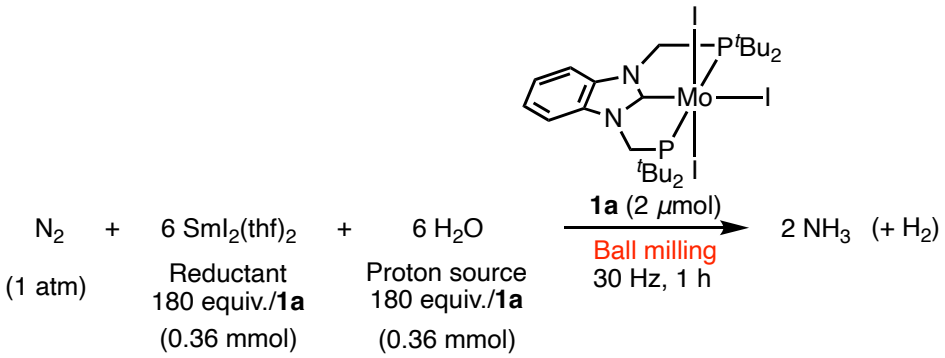

Entry	NH_3 (equiv./**1a**)	NH_3 (%)	H_2 (equiv./**1a**)	H_2 (%)
1[a]	29.5 ± 0.5	48	13.9 ± 3.7	15
2[b]	22	39	57	66
3[a,c]	27 ± 5	44	9 ± 2	11

[a]Data were mean of multiple individual experiments (at least 2) with error bars representing standard deviation.

[b]THF (49 μL, 300 equiv./Mo) was added as an additive. [c]stainless-steel balls (d = 5.0 mm × 8) were used.

Supplementary Table 2. Investigation of the proton sources.

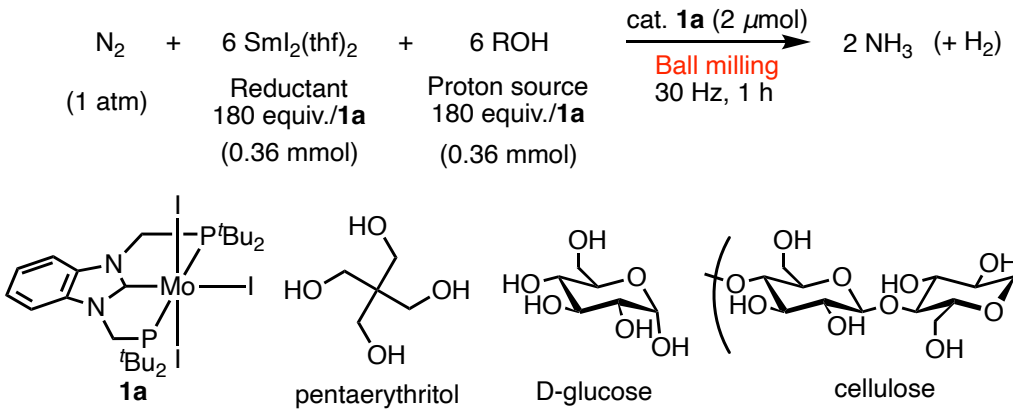

Entry	Proton source	m.p. (°C)	Solid/ Liquid	NH_3 (equiv./**1a**)	NH_3 (%)	H_2 (equiv./**1a**)	H_2 (%)
1[a]	H_2O	0	Liquid	29.5 ± 0.5	48	13.9 ± 3.7	15
2[a]	MeOH	−98	Liquid	10.3 ± 1.3	18	16.4 ± 1.8	19
3[a]	EtOH	−114	Liquid	21.9 ± 2.6	38	20.0 ± 1.6	23
4	^{i}PrOH	−89	Liquid	17	29	10	12
5	ethylene glycol	−13	Liquid	11.6	19	28.2	31
6[a]	$HO(CH_2)_3OH$	−27	Liquid	11 ± 0	18	9 ± 1	10
7	$HO(CH_2)_8OH$	62	Solid	11	17	14	16
8	$HO(CH_2)_{10}OH$	73	Solid	13	22	27	29
9[a]	pentaerythritol	261	Solid	48.9 ± 0.9	81	14.3 ± 6.6	16
10[a]	trimethylolethane	201	Solid	33 ± 9	51	18 ± 9	19
11[a]	neopentyl glycol	129	Solid	31 ± 1	54	13 ± 9	15
12	neopentyl alcohol	53	Solid	14	24	7	8
13	PhOH	41	Solid	22	35	8	8
14	catechol	105	Solid	32	53	32	35
15	oxalic acid	190	Solid	2	3	3	3
16	benzoic acid	122	Solid	<1	<1	3	3
17[a]	D-glucose	146	Solid	33.1 ± 3.6	56	1.8 ± 0.2	2
18	*β*-cyclodextrin	298	Solid	35.8	59	0	0
19[a]	cellulose	-	Solid	**43.5 ± 1.7**	**74**	0.6 ± 0.3	0.9

[a]Data were mean of multiple individual experiments (at least 2) with error bars representing standard deviation.

Supplementary Table 3. Effects of the number of hydroxy groups in a molecule to the ammonia formation.

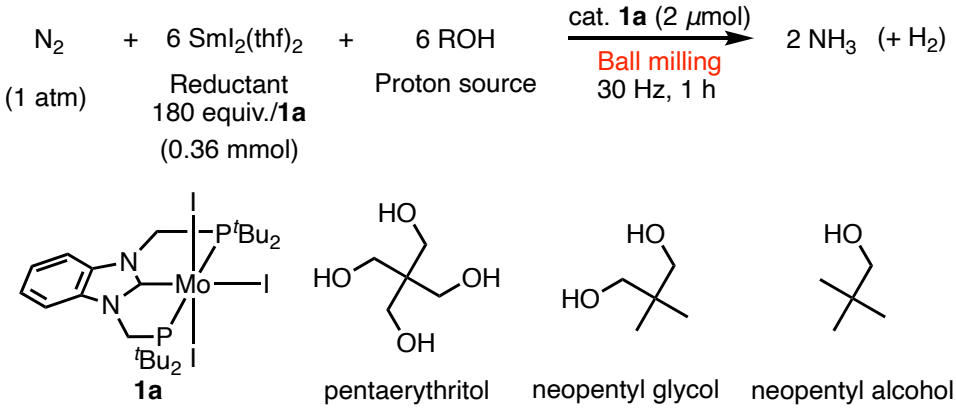

Entry	Proton source	Number of OH groups	x (mmol)	NH_3 (equiv./**1a**)	NH_3 (%)	H_2 (equiv./**1a**)	H_2 (%)
1[a]	pentaerythritol	4	0.18	**46 ± 4**	**79**	7 ± 2	8
2[a]	neopentyl glycol	2	0.36	31 ± 1	54	13 ± 0	15
3	neopentyl alcohol	1	0.72	17.9	31	15.1	18

[a]Data are the mean of multiple individual experiments (at least two) with error bars representing standard deviation.

Supplementary Table 4. Mechanochemical nitrogen fixation using cellulose and various molybdenum catalysts.

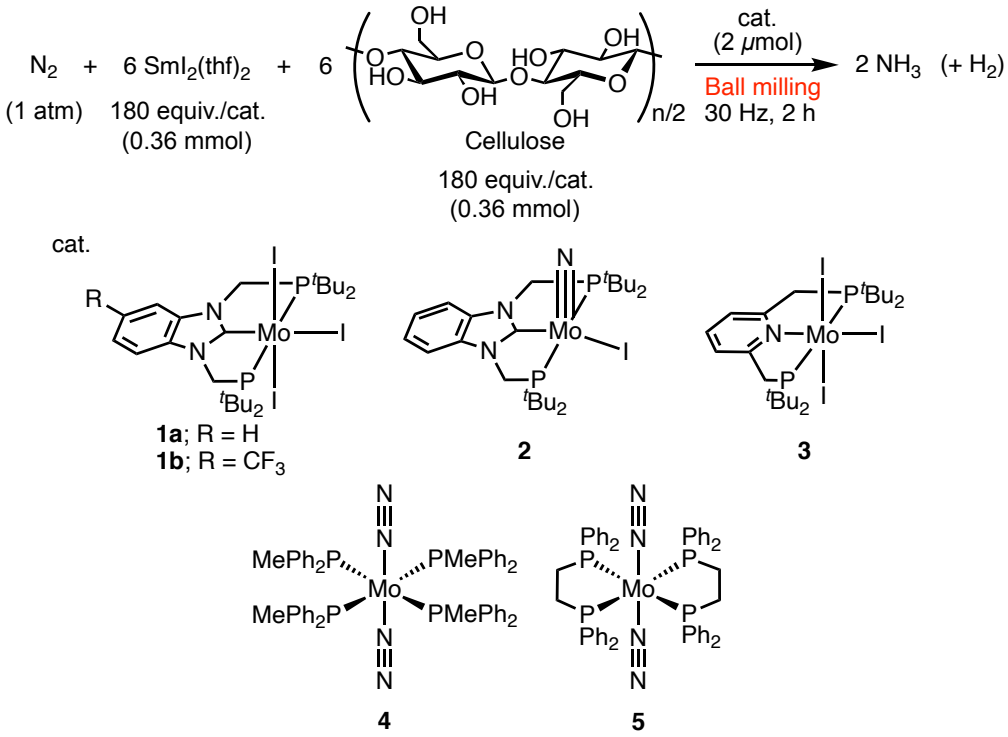

Entry	cat.	NH_3 (equiv./Mo)	NH_3 (%)	H_2 (equiv./Mo)	H_2 (%)
1[a]	**1a**	44 ± 2	74	0.5 ± 0.3	0.6
2	**1b**	47	76	0.5	0.5
3	**2**	46	81	0.7	0.8
4	**3**	33	37	0.4	0.3
5	**4**	0	0	2	2
6	**5**	6	10	7	8
7	Mo(0) Powder	0	0	0	0
8	MoO_3 Powder	0	0	0	0

[a]Data are the mean of multiple individual experiments (at least two) with error bars representing standard deviation.

Supplementary Table 5. Catalytic reduction of dinitrogen to ammonia with various concentration of 1a.

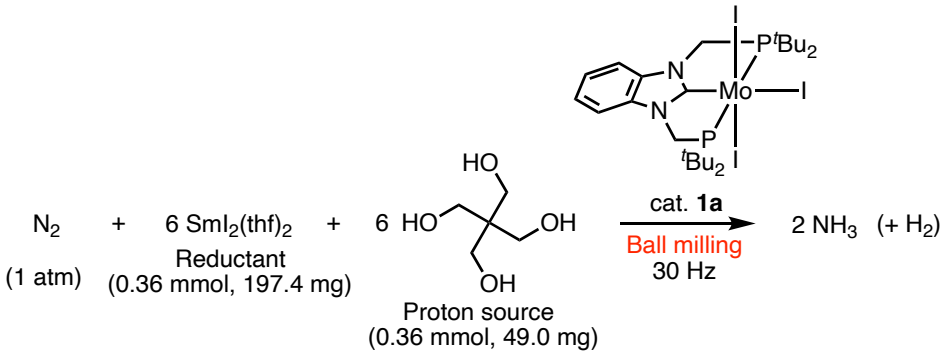

Amount of [**1a**] (μmol)	[**1a**] (mol/g)	log[**1a**]	Reaction time (min)	NH_3 (μmol)[a]	H_2 (μmol)[a]	v_{NH3} (μmol/g/h)[a]	log(v_{NH3})[a]
0.05	2.0×10^{-4}	−3.69	60	4.3	2.1	17.5	−4.76
0.1	4.1×10^{-4}	−3.39	60	55.1	14.3	224	−3.65
0.1	4.1×10^{-4}	−3.39	60	34.7	17.7	141	−3.85
			(average)	44.9 ± 10.2	16.0 ± 10.2	182 ± 41	−3.85 ± 0.10
0.2	8.1×10^{-4}	−3.09	15	34.3	17.7	556	−3.25
0.2	8.1×10^{-4}	−3.09	15	32.9	21.2	534	−3.27
			(average)	33.6 ± 0.7	19.5 ± 1.8	545 ± 11	−3.26 ± 0.01
0.3	1.2×10^{-3}	−2.91	10	33.8	21.7	821	−3.08
0.3	1.2×10^{-3}	−2.91	10	27.1	11.3	660	−3.18
			(average)	30.5 ± 3.4	16.5 ± 5.2	741 ± 82	−3.13 ± 0.05
0.5	2.0×10^{-3}	−2.69	5	22.9	7.9	1115	−2.95
0.5	2.0×10^{-3}	−2.69	5	19.6	7.3	955	−3.03
			(average)	21.3 ± 1.7	7.6 ± 0.3	1035 ± 80	−2.99 ± 0.03
1.0	4.1×10^{-3}	−2.39	4	27.0	7.2	1644	−2.78
1.0	4.1×10^{-3}	−2.39	4	26.8	4.8	1631	−2.79
			(average)	26.9 ± 0.1	6.0 ± 1.2	1638 ± 6	−2.79 ± 0.00
2.0	2.0×10^{-3}	−2.09	4	29.3	6.6	1784	−2.75
2.0	2.0×10^{-3}	−2.09	4	31.5	8.7	1918	−2.72
			(average)	30.4 ± 1.1	7.7 ± 1.1	1851 ± 67	−2.73 ± 0.02

[a]The mean values are shown with error bars based on standard deviation.

X-ray Crystallographic Studies.

Crystallographic data of dinuclear Sm(III)-pentaerythritol complex $[Sm(OHMe)(C_5H_{12}O_4)(C_5H_{11}O_4)]_2I_4\bullet(MeOH)_2$ is summarized in **Supplementary Table 6**. Its synthetic method and ORTEP drawings are shown in **Supplementary Figs. 18 and 19**, respectively. Diffraction data were collected for the 2θ range of 4° to 60° on a Rigaku XtaLAB Synergy-S diffractometer equipped with a HyPix-6000HE Hybrid Photon Counting (HPC) detector and VariMax optics using multi-layer mirror monochromated Mo $K\alpha$ radiation (λ = 0.71073 Å). Intensity data were corrected for Lorenz-polarization effects and for empirical absorption (CrysAlisPro), whereas structure solution and refinements were carried out by using the *Olex2* crystallographic software package.[S11] The positions of non-hydrogen atoms were determined by direct methods (SHELXT Version 2018/2[S12]) and subsequent Fourier syntheses (SHELXL Version 2019/2[S13]) and were refined on F_o^2 using all unique reflections by full-matrix least-squares with anisotropic thermal parameters.

According to the International Union of Crystallography checkCIF reports, the following Alert level B errors are reported for the crystallographic data:

PLAT213_ALERT_2_B Atom C11 has ADP max/min Ratio.

The alert (PLAT213_ALERT_2_B) is due to the disorder of the ligand. However, solving these disorders could not improve the structure, thus disorders were ignored.

PLAT971_ALERT_2_B Check Calcd Resid. Dens. 0.91Ang From Sm1.

PLAT971_ALERT_2_B Check Calcd Resid. Dens. 1.03Ang From Sm1.

PLAT973_ALERT_2_B Check Calcd Positive Resid. Density on Sm1.

These alerts are due to several minor disorders of the molecule, although such minor disorders were not solved here.

Supplementary Table 6. X-ray crystallographic Data for $[Sm(OHMe)(C_5H_{11}O_4)(C_5H_{12}O_4)]_2I_4$•$(MeOH)_2$

	$[Sm(OHMe)(C_5H_{11}O_4)(C_5H_{12}O_4)]_2I_4$•$(MeOH)_2$
CCDC number	2369997
chemical formula	$SmC_{12}H_{31}O_{10}I_2$
formula weight	739.52
dimensions of crystal, mm^3	0.20 × 0.15 × 0.15
crystal color, habit	colorless, block
crystal system	triclinic
space group	*P*−1
a, Å	9.7758(4)
b, Å	10.2140(4)
c, Å	11.9767(5)
α, deg	68.469(4)
β, deg	87.624(4)
γ, deg	86.210(4)
V, $Å^3$	1109.80(8)
Z	2
ρ_{calcd}, g cm^{-3}	2.213
F(000)	702
μ, cm^{-1}	54.68
temperature, °C	−180
trans. factors range	0.492–1.000
no. reflections measured	14779
no. unique reflections	5562 (R_{int} = 0.0454)
no. parameters refined	248
R_1 ($I > 2\ \sigma(I)$)[a]	0.0401
wR_2 (all data)[b]	0.1098
GOF (all data)[c]	1.024
max diff peak / hole, e $Å^{-3}$	+2.92 / −1.36

[a] $R_1 = \Sigma||F_o| - |F_c||/\Sigma|F_o|$.

[b] $wR_2 = [\Sigma w(F_o^2 - F_c^2)^2/\Sigma w(F_o^2)^2]^{1/2}$, $w = 1/[\sigma^2(F_o^2) + (qP)^2 + rP]$, $P = (\mathrm{Max}(F_o^2, 0) + 2\,F_c^2)/3$ [q = 0.0604; r = 3.2751].

[c] $\mathrm{GOF} = [\Sigma w(F_o^2 - F_c^2)^2/(N_o - N_{params})]^{1/2}$.

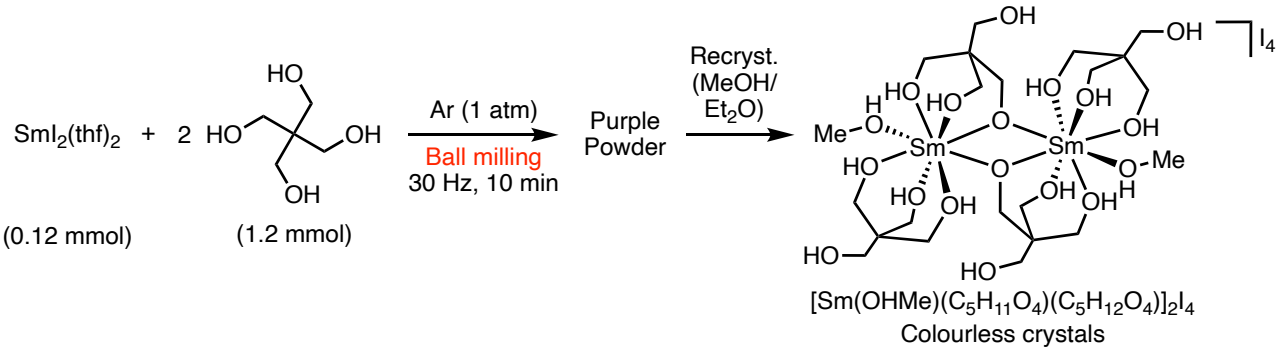

Supplementary Fig. 18 | Synthesis of dinuclear Sm(III)-pentaerythritol complex.

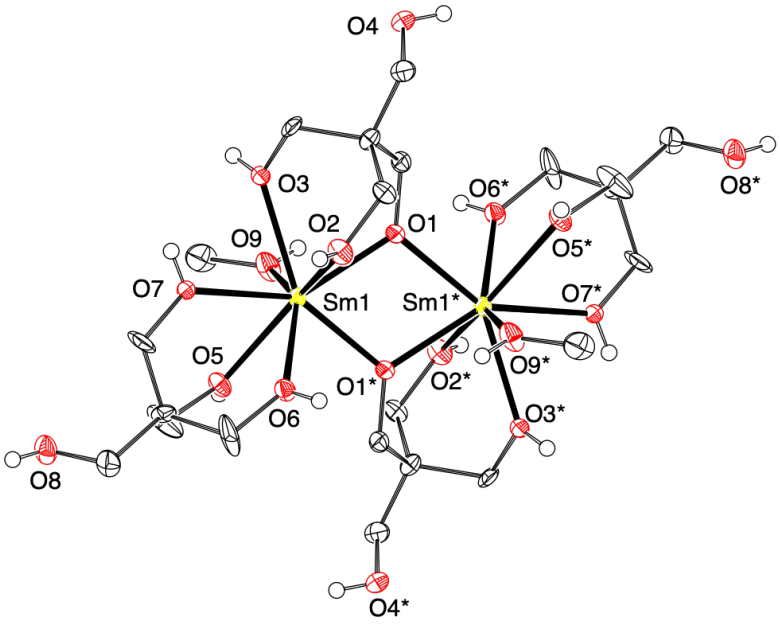

Supplementary Fig. 19 | ORTEP drawing of $[Sm(OHMe)(C_5H_{11}O_4)(C_5H_{12}O_4)]_2I_4 \cdot (MeOH)_2$. Thermal ellipsoids are shown at the 50% probability level, and hydrogen atoms attached to carbon atoms, solvent molecules, and counter anions are omitted for clarity.

References.

S1. Weatherburn, M. W. Phenol-hypochlorite reaction for determination of ammonia. *Anal. Chem.* **39**, 971–974 (1967).

S2. Watt, G. W. & Chrisp, J. D. Spectrophotometric method for determination of hydrazine. *Anal. Chem.* **24**, 2006–2008 (1952).

S3. Hvoslef, J. A neutron diffraction study of pentaerythritol. *Acta Crystallogr.* **11**, 383–388 (1958).

S4. Eizawa, A. *et al.* Catalytic reactivity of molybdenum–trihalide Complexes bearing PCP-type pincer ligands. *Chem. – Asian J.* **14**, 2091–2096 (2019).

S5. Ashida, Y. *et al.* Catalytic production of ammonia from dinitrogen employing molybdenum complexes bearing N-heterocyclic carbene-based PCP-type pincer ligands. *Nat. Synth.* **2**, 635–644 (2023).

S6. Arashiba, K. *et al.* Catalytic nitrogen fixation via direct cleavage of nitrogen–nitrogen triple bond of molecular dinitrogen under ambient reaction conditions. *Bull. Chem. Soc. Jpn.* **90**, 1111–1118 (2017).

S7. Lazarowych, N. J., Morris, R. H. & Ressner, J. M. Spectroscopic and chemical properties of nitrogen-15-enriched molybdenum dinitrogen complexes *trans*,*mer*-$Mo(N_2)_2(L)(PMePh_2)_3$. *Inorg. Chem.* **25**, 3926–3932 (1986).

S8. Hussain, W., Leigh, G. J., Ali, H. Mohd., Pickett, C. J. & Rankin, D. A. Dinitrogen binding and electrochemistry in complexes of molybdenum and tungsten. *J. Chem. Soc. Dalton Trans.* 1703–1708 (1984).

S9. Watson, P. L., Tulip, T. H. & Williams, I. Defluorination of perfluoroolefins by divalent lanthanoid reagents: activating carbon-fluorine bonds. *Organometallics* **9**, 1999–2009 (1990).

S10. Ravel, B. & Newville, M. *ATHENA* , *ARTEMIS* , *HEPHAESTUS* : data analysis for X-ray absorption spectroscopy using *IFEFFIT*. *J. Synchrotron Radiat.* **12**, 537–541 (2005).

S11. Dolomanov, O. V., Bourhis, L. J., Gildea, R. J., Howard, J. A. K. & Puschmann, H. *OLEX2* : a complete structure solution, refinement and analysis program. *J. Appl. Crystallogr.* **42**, 339–341 (2009).

S12. Sheldrick, G. M. *SHELXT* – Integrated space-group and crystal-structure determination. *Acta Crystallogr. Sect. Found. Adv.* **71**, 3–8 (2015).

S13. Sheldrick, G. M. Crystal structure refinement with *SHELXL*. *Acta Crystallogr. Sect. C Struct. Chem.* **71**, 3–8 (2015).